EARLINET Single Calculus Chain – technical Part 2: Calculation of optical products

Ina Mattis[1], Giuseppe D'Amico[2], Holger Baars[3], Aldo Amodeo[2], Fabio Madonna[2], and Marco Iarlori[4]

[1]Deutscher Wetterdienst, Meteorologisches Observatorium Hohenpeißenberg, Albin-Schwaiger-Weg 10, 82383 Hohenpeißenberg, Germany
[2]Consiglio Nazionale delle Ricerche - Istituto di Metodologie per l'Analisi Ambientale (CNR-IMAA), Contrada S. Loja - Zona Industriale, 85050 Tito Scalo (Potenza), Italy
[3]Leibniz Institute for Tropospheric Research, Permoserstr. 15, 04318 Leipzig, Germany
[4]CETEMPS - Dipartimento di Scienze Fisiche e Chimiche, Università Degli Studi - L'Aquila, Via Vetoio Località Coppito, 67010 L'Aquila, Italy

Correspondence to: I. Mattis
(ina.mattis@dwd.de)

Abstract. In this paper we present the automated software tool ELDA (EARLINET Lidar Data Analyzer) for the retrieval of profiles of optical particle properties from lidar signals. This tool is one of the calculus modules of the EARLINET Single Calculus Chain (SCC) which allows for the analysis of the data of many different lidar systems of EARLINET in an auto-mated, unsupervised way. ELDA delivers profiles of particle extinction coefficients from Raman signals as well as profiles of

5 particle backscatter coefficients from combinations of Raman and elastic signals or from elastic signals only. Those analyses start from pre-processed signals which have already been corrected for background, range dependency and hardware specific effects. An expert group reviewed all algorithms and solutions for critical calculus subsystems which are used within EAR-LINET with respect to their applicability for automated retrievals. Those methods have been implemented in ELDA. Since the software was designed in a modular way, it is possible to add new or alternative methods in future. Most of the implemented

10 algorithms are well known and well documented, but some methods have especially been developed for ELDA, e.g., automated vertical smoothing and temporal averaging or the handling of effective vertical resolution in case of lidar ratio retrievals, or the merging of near-range and far-range products. The accuracy of the retrieved profiles was tested following the procedure of the EARLINET-ASOS algorithm inter-comparison exercise which is based on the analysis of synthetic signals. Mean de-viations, mean relative deviations, and normalized root-mean-square deviations were calculated for all possible products and

15 three height layers. In all cases, the deviations were clearly below the maximum allowed values according to the EARLINET quality requirements.

1 Introduction

Lidars are an excellent tool to study vertical profiles of different aerosol properties. But before the year 2000, lidar data sets were mostly limited to observations at only few stations and short term field campaigns. The situation changed, when EARLINET

20 (European Aerosol Research Lidar NETwork) was established in 2000 as a coordinated lidar network on continental scale

(Bösenberg et al., 2003) with the goal to establish a long-term systematic observation of the vertically resolved aerosol distribution over Europe. EARLINET consists of research lidars which have originally been designed for many different purposes. These instruments cover a large range with respect to complexity, temporal and range resolution, and vertical measurement range (Pappalardo et al., 2014; Freudenthaler et al., 2016). Thus, there are as many different analysis tools as distinct lidar systems in the network. Most of them were designed for manual operation. They are individually optimized for the corresponding lidar instrument. EARLINET put large effort into the development of quality standards on instrument and hardware level in order to ensure a homogeneous level of data quality. The primary goal of EARLINET is to deliver high-quality climatological data within 6 months after the measurement according to EARLINET rules.

Beside the need for high-quality climatological aerosol profile data, an upcoming and increasing need for faster delivery and higher availability of such data is arising, e.g. for the study of transport events or for data assimilation in air quality forecasting models. Therefore, one of the major goals of the EARLINET-ASOS (EARLINET Advanced Sustainable Observation System) project (2006-2011) was to develop a single calculation chain (SCC) which allows for an analysis of the raw lidar data of all the different EARLINET lidar instruments in an automated, unsupervised way in order to speed up data analysis and data availability and to improve the homogeneity of the delivered data due to the use of only one single algorithm (D'Amico et al., 2015a). The case of the eruption of Eyjafjallajökull volcano in Iceland 2010 demonstrated the need for such an automated tool for fast and coordinated data delivery. Unfortunately, the SCC was not yet finished at that time and thus, the publication of scientifically quality assured EARLINET data of this event lasted 2 years (Pappalardo et al., 2013). Meanwhile, the SCC has become available and Sicard et al. (2015) demonstrated its ability to deliver backscatter and extinction profiles in near real-time during an intense field campaign in the Mediterranean basin in summer 2012.

SCC consists of different modules (D'Amico et al., 2015a). The pre-processor module ELPP (EARLINET Lidar Pre-Processor) applies many different corrections to the raw lidar signals before they can be used to derive profiles of optical aerosol properties (D'Amico et al., 2015b). Those are general corrections, like range correction, or hardware specific corrections, like trigger delay correction. ELPP also determines and provides data for atmospheric corrections like the correction for atmospheric transmission due to molecular scattering. The task of the optical processor module ELDA (EARLINET Lidar Data Analyzer) is to retrieve profiles of optical aerosol properties from the pre-processed signals. The SCC database is used for the handling of all input parameters and contains technical descriptions of the instruments. A daemon software automatically starts the ELPP and ELDA modules. Finally, a user friendly web-interface is provided to upload the raw signal files, access to all input parameters and download the pre-processed and processed data.

The general applicability of the overall SCC and of ELDA algorithms to signals from different lidar systems is demonstrated in D'Amico et al. (2015a) and Wandinger et al. (2015) using data that have been obtained during the EARLINET instrument inter-comparison campaign at Leipzig in 2009 (EARLI09). The accuracy of SCC products with respect to manually analyzed profiles has been validated using long-term observations under different meteorological situations (D'Amico et al., 2015a). This paper focuses on tests of the performance of the overall SCC and of ELDA in terms of accuracy. Those tests have been performed by analyzing the synthetic lidar signals which were generated for the EARLINET-ASOS algorithm inter-comparison

exercise (Böckmann and Pappalardo, 2007; EARLINET-ASOS, 2011) based on the methodology described in Pappalardo et al. (2004).

This paper is the third in a series of three publications about the SCC. The general structure of SCC is described by D'Amico et al. (2015a). D'Amico et al. (2015b) provide a detailed description of the SCC pre-processor module. The focus of this paper is

5 on the description of the SCC module for the retrieval of profiles of optical aerosol properties ELDA. It provides an overview on all implemented standard algorithms together with a full documentation of methods which have specially developed for ELDA. Whenever SCC derived EARLINET data will be used in future scientific studies, this general documentation will be a very useful tool for the understanding and interpretation of the data.

This paper is structured as follows: Section 2 provides a general overview on ELDA, including a list of possible products.

10 This section explains the procedure of selection of implemented algorithms and provides a specification of ELDA's interfaces to other SCC modules, and a description of the technical implementation. Section 3 provides a summary of ELDA's methods and algorithms which are already well known, well documented, and well tested (standard algorithms). Methods and algorithms which have especially developed or adopted for ELDA are described in section 4. Those are the handling of effective vertical resolution in case of lidar ratio calculation (4.2), the merging of product profiles in case of measurements with near-range and

15 far-range telescope (4.3), and the automated vertical smoothing and temporal averaging (4.1). The results of the validation of ELDA with the tools of the EARLINET algorithm inter-comparison exercise are presented in section 5. Finally, section 6 provides a summary of this paper.

2   EARLINET Lidar Data Analyzer (ELDA)

The optical processor module of SCC (ELDA) retrieves profiles of optical aerosol properties from the pre-processed signals.

20 Those are grouped into the following product types:

- **elastic backscatter coefficient:** profile of particle backscatter coefficient β that is derived from an elastic signal only (Klett, 1981; Fernald, 1984; Di Girolamo et al., 1999; Masci, 1999),

- **Raman backscatter coefficient:** profile of particle backscatter coefficient that is derived from a combination of an elastic signal and a Raman signal (Ansmann et al., 1992b; Ferrare et al., 1998),

25 - **extinction coefficient:** (in SCC web-interface referred to as 'extinction only'): profile of particle extinction coefficient α which is calculated with the Raman method (Ansmann et al., 1990, 1992a), and

- **lidar ratio:** (in SCC web-interface referred to as 'lidar ratio and extinction') which consists of a particle extinction profile and the corresponding particle backscatter profile, both obtained with the Raman method and with the same effective vertical resolution. This product allows for the calculation of a profile of the particle lidar ratio S.

30 Profiles of backscatter coefficients are typically calculated with high vertical resolution. They are inserted into the *b files* of the EARLINET database (Pappalardo et al., 2014). Profiles of particle extinction coefficients typically have a lower vertical

resolution. Extinction coefficients and lidar-ratio products both can be found in the *e files* as defined for the EARLINET database.

2.1 Selection of implemented methods and algorithms

The SCC module ELDA was developed as a software package that is able to retrieve aerosol properties in an automatic way
5 and without the need for operator interaction. As a first step in the development of this software package, an expert group has compiled a list of calculus subsystems which might be difficult to handle or for which different solutions are used within EARLINET. Those critical calculus subsystems are:

1. in the calculation of extinction coefficients:

    (a) the calculation of the derivative,
10 (b) the estimation of the uncertainty of the derived extinction,
    (c) the determination of the overlap function and of the height of complete overlap, and
    (d) the assumption of the Ångström exponent;

2. in the calculation of Raman backscatter coefficients:

    (a) the detection of the calibration height or height range and
15 (b) the estimation of the calibration value;

3. in the calculation of elastic backscatter coefficients:

    (a) the assumption of the unknown profile of the particle lidar ratio and
    (b) the determination of the overlap function and of the height of complete overlap;

4. the general handling of vertical smoothing and temporal averaging.

20 Next, a survey was performed among the EARLINET groups in order to compile a list of all algorithms used in the community and to collect individual solutions of the critical calculus subsystems. Finally, all reported algorithms and methods have been reviewed by the expert group with respect to their general applicability for the automated algorithms of the SCC software. If several suitable solutions for one specific problem are widely used in the community, they were implemented in the software code as parallel options allowing the user to choose among them. This is the case e.g. for the retrieval of uncertainties where the
25 user has the choice between the options 'Monte-Carlo' and 'error of the used method (error propagation)'. Table 1 provides an overview on all implemented products with their optional methods of retrieval and error estimation. Further, it was decided to design the SCC software in a modular way that is easily possible to implement additional algorithms or new optional methods in future.

2.2 Interfaces

Figure 1 in D'Amico et al. (2015a) illustrates the general structure of the SCC and the interfaces that connect ELDA to the other modules of the SCC.

Main source of data input to ELDA are intermediate files in NetCDF format (http://www.unidata.ucar.edu/software/netcdf/docs) which are produced by ELPP. They contain signal data which were corrected for atmospheric and electronic background and range-dependency. A value of statistical uncertainty is attributed to each data point. System specific corrections like dead-time correction or overlap correction are already applied by ELPP to these signals as well. The pre-processed signals have been re-sampled to an uniform time and range resolution. Additionally, the intermediate files contain the corresponding profiles of atmospheric transmission due to molecular scattering, profiles of the molecular scattering coefficients, and profiles of cloud flags. The cloud-flag profiles are actually provided by the user within the SCC raw files. A new module for automated cloud-masking will be implemented into the SCC within the ACTRIS-2 (Aerosol, Clouds and Trace gases Research InfraStructure) project (http://www.actris.eu). The user can provide input parameters for the data analysis that change frequently (e.g., the actual lidar ratio) to the SCC within the raw input signal files. This information is transferred by ELPP to ELDA within the intermediate NetCDF file. Each of these intermediate files contains all necessary information which can be provided by ELPP for the retrieval of one individual product. If several products shall be derived by ELDA, separate intermediate files have to be prepared by ELPP for each of them. All profiles corresponding to a particular product are delivered with the same, user-defined sampling interval. For example, if an extinction profile shall be retrieved from a combination of signals from different telescopes, both the near-range and the far-range signals are delivered with the same sampling interval.

The relational SCC database is used to store system specific parameters and product calculation options which do not change from measurement to measurement like the height range in which the products typically can be derived or the maximum statistical uncertainty that shall be achieved by the retrievals.

The results obtained by ELDA are written in NetCDF files. The format of these *b files* and *e files* strictly follows the EARLINET rules (see http://www.earlinet.org). Beside the required information, they contain new additional variables and attributes, e.g. the measurement ID, information on cloud-flag profiles, and profiles of the automatically obtained vertical resolution. ELDA products are always provided with the same sampling interval as the sampling interval of the pre-processed signals.

The SCC daemon module automatically starts ELDA as soon as there are pre-processed signals of a new measurement available. The daemon also monitors the exit status of ELDA and informs the user about success or failure of the current ELDA run.

The products of the SCC can be derived in different ways depending on the complexity of the used lidar system. For example, particle backscatter coefficients can be calculated from a single signal only, or from a combination of signals from different telescopes or from a combination of signals containing different polarization components. Many different *use cases* describe all possible ways to retrieve a product from one or from a combination of several signals. They also describe, whether the signal combination needs to be performed in ELPP or in ELDA (D'Amico et al., 2015b).

2.3 General technical aspects of ELDA

ELDA is a command line application that has been developed with the platform independent compiler language Free Pascal [http://www.freepascal.org/]. Free Pascal is a 32 and 64 bit Pascal compiler for several processors, e.g., Intel x86, Amd64/x86 64, PowerPC, PowerPC64, Sparc, or ARM. Free Pascal can be used on many popular operating systems like for instance Linux,

5   Mac OS, DOS, Win32, Win64. Programs developed with Free Pascal compile on any platform. Since the Compiler is the same for all platforms it produces equivalent products (executables) for different platforms without any recoding. Free Pascal is freely available. Its packages and runtime library come under a modified Library GNU Public License (LGPL).

ELDA requires a database which operates on a MySQL database server version 4.0 to 5.5. MySQL is an open source software for Windows and Unix/Linux [http://www.mysql.com]. Further, MySQL and NetCDF libraries corresponding to the operating

10   system are required.

When operated as module of the SCC, ELDA is started by the SCC daemon software automatically as soon as there are new intermediate NetCDF files available which have been produced by the pre-processing module. There is also the option to start ELDA individually at command line by the command:

$>$ elda M [-c $config\_file$]

15   The mandatory parameter M is the measurement ID of the lidar observation which should be processed, with the optional parameter $config\_file$ one can provide the location of a configuration file. If this parameter is not provided, a configuration file must be provided at the actual working directory. The configuration file contains parameters like database connection data or paths of input, output, and log data.

ELDA was written with an object oriented structure. Main classes are product factories and data profiles. When ELDA

20   is started, instances of product factories are created for each scheduled product type and wavelength. Those factories load intermediate NetCDF files and product calculation options from the SCC database, calculates extinction and/or backscatter profiles, applies automatically vertical smoothing and temporal averaging, and finally, store the profiles in EARLINET NetCDF format.

ELDA comes with a logging system which allows for writing log files with variable, user defined log levels. A log file is

25   generated for each analyzed measurement. The log level can range from 'llQuiet' (no log output) to 'llDebug' (all messages are logged).

3 Standard algorithms implemented in ELDA

All retrieval algorithms implemented in ELDA are well known in the lidar community, well documented in various publications and well tested in many applications. Thus, the following sections do not provide detailed descriptions of the implemented

30   formulas. Instead, details of the implementation, especially of the critical calculus subsystems, and user adjustable parameters are explained.

3.1 Calculation of particle backscatter coefficient

One critical subsystem in the retrieval of particle backscatter coefficients (with any method) occurs if the corresponding lidar system detects parallel ($P^\parallel$) and cross polarized ($P^\perp$) components of elastically backscattered signals in separate channels. Before those signals can be used for backscatter retrievals, they are combined in ELDA into a total signal using the formula

$$P = P^\parallel + F_\delta \, P^\perp. \tag{1}$$

The depolarization factor F_δ needs to be provided by the user in the corresponding SCC raw signal file and is provided to ELDA in the intermediate file. This factor represents the simplest form of the calibration factor for the retrieval of the volume depolarization ratio $\delta = F_\delta \, P^\perp / P^\parallel$. Actually, a new module of SCC is under development, which will automatically performs the depolarization calibration if the user submits a calibration measurement which is obtained with the $\Delta 90°$ method (Freudenthaler, 2015). The next version of ELDA will be able to handle those more sophisticated calibration data.

3.1.1 Raman backscatter

In the assessment report of existing calculus subsystems used within EARLINET (Mattis et al., 2007) was found that two different methods to derive Raman backscatter coefficients are used. Both methods are based on the same idea, have the same advantages and sources of uncertainty. They differ only in the way to perform the mathematical calculations.

The methodology as described by Ferrare et al. (1998) calculates the backscatter coefficient β via the backscatter ratio. It was implemented as standard algorithm in ELDA. The calibration value has to be provided in terms of backscatter ratio (which has a value of 1 in ideal aerosol free conditions). The original algorithm of Ansmann et al. (1992b) is foreseen as alternative method in the code, but was not yet fully implemented. The calibration value for this method would have to be provided in terms of particle backscatter coefficient (which has a value of $0\,\mathrm{m}^{-1}\mathrm{sr}^{-1}$ in ideal aerosol free conditions). Details of the calibration procedure and its parameters are explained in section 3.1.3.

3.1.2 Elastic backscatter coefficient

Also for the retrieval of backscatter coefficient from elastic signals, the EARLINET partners use two different methods. Those are the iterative method (Di Girolamo et al., 1999; Masci, 1999) and the Klett-Fernald algorithm in backward integration mode (Klett, 1981; Fernald, 1984) . Both methods are implemented in ELDA and the user has to choose among them. Both methods require the input of a profile of particle lidar ratio S. If available, the user may provide a S profile as an ancillary file together with the raw data file of the corresponding measurement. This information is then passed by ELPP via the intermediate file to ELDA. In most cases, an appropriate S profile is not available. For such circumstances, the user can provide a single, typical S value in the SCC database or raw data file that is used by ELDA for the whole profile.

In the iterative method, profiles of the particle backscatter coefficient are calculated with the Raman method that is implemented in ELDA. Instead of the measured Raman signal, here we use a virtual molecular signal that is simulated in each iteration step i from the profile of the molecular scattering coefficient and from the profile of the particle backscatter coeffi-

cients of the previous step $\beta^{\mathrm{par}}_{(i-1)}$. For the initial step, the molecular signal is calculated with the assumption that the particle backscatter coefficient is equal to zero at all heights. The iteration is finished successfully if the absolute value of the relative distance $\delta^{\beta}_{(i)}$ between the backscatter profiles of two subsequent iterations steps is below a certain percentage threshold. The convergence criterion $\delta^{\beta}_{(i)}$ is defined as

$$5 \quad \delta^{\beta}_{(i)} = \left| \frac{\int \beta^{\mathrm{par}}_{(i)} - \int \beta^{\mathrm{par}}_{(i-1)}}{\delta^{\beta}_{(i-1)}} \right|. \tag{2}$$

The process is finished successfully as soon as the convergence criterion is fulfilled or it is aborted returning an error exit code when a maximum number of iteration steps was performed without meeting the convergence threshold. The user can provide the maximum number of iteration steps and the convergence threshold in the SCC database as parameters to ELDA. Typical values are 10 steps and 0.01 (1%).

10   The convergence criterion in equation 2 is a relative value that describes how the relative distance between subsequent backscatter profiles changes from step to step. As an advantage of this definition, the threshold of $\delta^{\beta}_{(i)}$ is a percentage value that does not depend on the magnitude of the actual backscatter values. Thus, the same threshold can be used for retrievals at different wavelengths or for different meteorological situations which might be characterized by very different values of $\int \beta^{\mathrm{par}}_{(i)}$. For the calculation of the difference between backscatter profiles ELDA uses the integrated values. Those are less influenced
15   by statistical uncertainties than individual points of the backscatter profile. Integrals are calculated between minimum and maximum height of the corresponding product (see section 3.4).

3.1.3 Handling of backscatter calibration

All methods of calculating profiles of particle backscatter coefficients include a certain calibration procedure. Usually a particle-free region in the free troposphere r_{ref} with $\beta^{\mathrm{par}}(r_{ref}) = 0$ is used for calibration. ELDA is searching automatically
20   for such a region. It searches for an altitude region where

- the elastically backscattered signal in case of Klett-Fernald method,

- the ratio between the elastically backscattered signal and Raman signal in case of Raman method, or

- the ratio between the elastically backscattered signal and the virtual molecular signal in case of iterative method

are minimum. A calibration window of user defined width is shifted through the altitude region, where particle-free conditions
25   typically occur (user defined calibration interval). For each window position, the average and standard deviation of the signal or signal ratio is calculated. It is assumed that the window position where the signal or signal ratio has its minimum is closest to the assumed particle-free conditions. The average value within this calibration window and its standard deviation are used to estimate the calibration factor and its statistical uncertainty. If the user knows from ancillary data, e.g., from sun-photometer observations or from climatological data of the stratospheric particle load, that there is no particle-free altitude layer, it is
30   possible to provide backscatter ratios different from 1 as calibration value. Windows with standard deviations larger than the

user defined maximum allowable statistical error (see section 4.1) are not used for calibration. From this reason, it may happen that no valid calibration window can be found if the signal-to-noise ration within the calibration interval is strongly reduced, e.g., due to clouds in lower parts of the profile.

This method has the disadvantage to not guarantee that in the calibration window there are no particles at all. The algorithm would find a minimum also in case that there are only less particles than in other altitude regions. This uncertainty may cause large errors in the retrieved backscatter profiles. A further, stronger criterion to find particle free regions would be a test whether the measured signals have the same shape like a theoretically assumed Rayleigh signal. It is planned to implement a better method to search for a proper calibration window that applies different statistical tests to ensure that the shape of the tested signal corresponds to the shape of a Rayleigh signal.

3.1.4 Comparison of different backscatter methods

Figure 1 illustrates the results of the different alternative backscatter retrieval methods based on the synthetic signals at 532 and 607 nm that have been provided within EARLINET in the framework of the algorithm inter-comparison exercise (Böckmann and Pappalardo, 2007; EARLINET-ASOS, 2011). All products have been retrieved with the same calibration parameters. Details of the calibration procedure are explained in paragraph 3.1.3. The calibration window of 1 km width has to be found automatically within the calibration interval which is between 5 and 10 km altitude. All ELDA results agree very well with the input data (black line) with mean deviations smaller than $1 \times 10^{-7} \mathrm{m}^{-1}\mathrm{sr}^{-1}$. Best agreement is achieved with the Raman method (mean relative deviations less than 10%), followed by the Klett-Fernald algorithm (mean relative deviations less than 15%) and the iterative method (mean relative deviations up to 30%). Solid red and green lines have been obtained with the assumption of an altitude independent particle lidar ratio value of 62 sr which is the mean value of the input particle lidar ratio profile of the simulation. The effective vertical resolution and relative statistical errors of all three methods are nearly equal.

3.2 Calculation of particle extinction coefficient

ELDA calculates profiles of particle extinction coefficients with the Raman method (Ansmann et al., 1990, 1992a) from pre-processed Raman signals. Those signals are already corrected for incomplete overlap, background, range dependency and other system specific effects. In a first step, ELDA corrects the pre-processed signals for atmospheric transmission due to molecular extinction. Profiles of atmospheric transmission at emitted wavelength and at Raman shifted wavelengths are also provided by ELPP in the intermediate files. In the current version of ELDA, the user has the choice to calculate the derivative of the pre-processed signals by weighted or non-weighted linear fit method. In case of weighted linear fit, uncertainties of individual data points are not taken into account when calculationg the linear fit. In case of weighted linear fit, data points with larger uncertainties have less weight than data points with lower uncertainties within the calculation of the linear fit (Press et al., 1992). Some groups in EARLINET use other methods for the retrieval of the derivative (Pappalardo et al., 2004; Iarlori et al., 2015). The implementation of these methods is prepared in the code, but not yet completely realized.

If the user decides to obtain an *extinction only* product, only the profile of the particle extinction coefficient is retrieved and exported to a NetCDF file together with the profile of its statistical error and effective vertical resolution according to
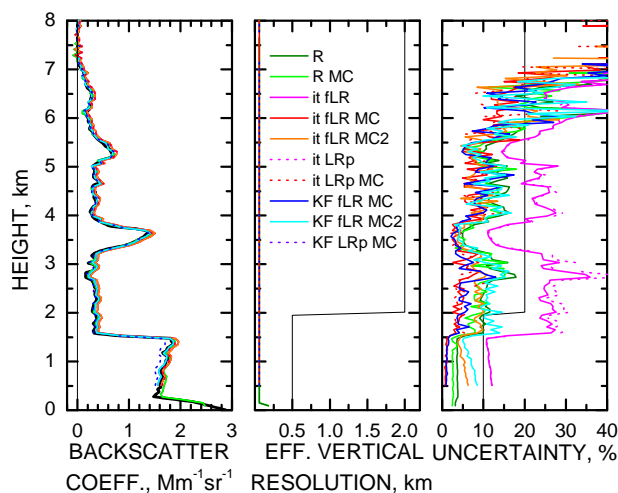
Figure 1. Profiles of the particle backscatter coefficient at 532 nm (left panel), its effective vertical resolution (center panel), and relative statistical uncertainties (right panel). The colored lines show the results of ELDA corresponding to the different tested methods which identified in the legend by short id's (See table 1 for full descriptions of the tested methods). The bold black line in the left panel shows the input data of the algorithm inter-comparison exercise. The Raman backscatter profile was obtained with automated smoothing. All other profiles were calculated with the vertical resolution of the pre-processed signals of 60 m. Thin black lines indicate the general constraints of all retrievals. Maximum allowable smoothing was 500 m and 2 km below and above 2 km altitude, respectively (center). Maximum allowable relative errors were 10% and 20% below and above 2 km, respectively (right).

EARLINET format of *e files*. If the product *lidar ratio and extinction* is selected, ELDA additionally calculates with the Raman method a profile of particle backscatter coefficient which has the same effective vertical resolution as the extinction profile. In this case, the derived *e file* contains the extinction and backscatter profiles together with their statistical errors and the effective vertical resolution profile.

Figure 2 illustrates the results of the different alternative extinction retrieval methods based on the synthetic signals at 607 nm that have been provided within EARLINET in the framework of the algorithm inter-comparison exercise (Böckmann and Pappalardo, 2007; EARLINET-ASOS, 2011). All profiles have been vertically smoothed with ELDA's automated procedure (see section 4.1) with the constraints of maximum allowable relative statistical uncertainties of 20% and 50% below and above 2 km height, respectively. As in case of backscatter retrievals, all ELDA extinction profiles agree very well with the input data (black line) with mean relative deviations smaller than 15%. The uncertainty profiles and profiles of vertical resolution show also a good agreement.

3.3 Estimation of statistical uncertainties

For all products and retrieval algorithms, the user can choose whether the statistical uncertainties shall be calculated with the Monte Carlo method or by means of error propagation. The only exception are retrievals with the Klett-Fernald algorithm for

which the estimation of uncertainties is implemented only with Monte Carlo method, but not with error propagation. If the user decided to use the Monte Carlo method, the number of iterations can be set for each product individually. All examples in this paper have been calculated with 30 iterations. This number is a compromise between saving calculus time and accuracy of the retrieved error bars.

5   The Monte Carlo (MC) method is based on the random generation of new lidar signals. Each range bin of these signals is considered as a sample element of a Gauss probability distribution with mean value and standard deviation that corresponds to the value and uncertainty of the pre-processed signal profiles. The extracted lidar signals are then processed with the same algorithm to produce a set of solutions. The standard deviation of these solutions is finally used as profile of the statistical error. The product data values are independently calculated with the same algorithm, but from the original signal. ELDA uses

10   the random generator that is implemented in the Free Pascal compiler. The generator is initialized for the calculation of each individual product profile.

    ELDA applies automated smoothing procedures to all products (see section 4.1). In case of Monte Carlo error estimation, the automated smoothing is applied only ones from the original signal. Then, all individual Monte Carlo solutions are obtained with the profile of vertical resolution which was derived from the original signal. This procedure ensures that all Monte Carlo

15   samples have the same effective vertical resolution before the standard deviation is calculated.

    In case of backscatter retrievals, the calibration procedure in ELDA is performed independently for each sample signal. Thus, the resulting error profile contains also the statistical calibration uncertainty. There is also the option to provide an uncertainty value of the assumed particle lidar ratio in case of backscatter retrievals from elastic signals only. This S uncertainty is handled by the Monte Carlo procedure in the same way as the signal errors. The right panel of Figure 1 illustrates this feature. The

20   blue curve shows the statistical error of the particle backscatter coefficient derived by the Klett-Fernald algorithm when the Monte Carlo methods takes only the signal errors into account. In comparison, the cyan curve shows the resulting error profile when an additional uncertainty of $10\,\mathrm{sr}$ is assumed for the particle lidar ratio. It can be seen that the difference between both error profiles increases with decreasing altitude and increasing distance to the calibration point. The consideration of the S uncertainty causes an uncertainty of the particle backscatter coefficient in the lower part of the profile which is up to 10%

25   larger than without S uncertainty.

    It can be seen from the comparison between the green and olive curves in the right panels of Figure 1 and of Figure 2 that the Monte Carlo method (green) and error propagation (olive) provide comparable error profiles in case of Raman extinction and Raman backscatter retrievals. The situation is different in case of the backscatter retrieval with the iterative method. Here, the results of error propagation (magenta curve in right panel of Figure 1) are much larger than the results of the corresponding

30   Monte Carlo retrievals (red curve). This is due to the fact that the influence of the signal errors is amplified within each iteration step. Therefore, it is recommended to use the Monte Carlo algorithm for the error retrieval of the iterative method.

    Especially the agreement of uncertainties in case of the extinction retrieval is a verification that error estimates in the SCC work well because the uncertainties of both methods are derived independent of each other. In case of extinction retrieval by non-weighted linear fit, the signal uncertainties are not included in the fitting procedure. The extinction value is calculated from

35   the slope parameter of the fitted linear function. The extinction uncertainty is directly derived from the uncertainty of the slope
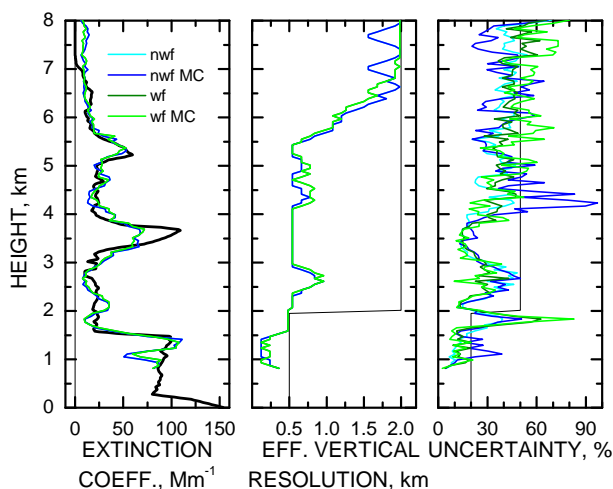
Figure 2. Same as figure 1, but for profiles of the particle extinction coefficient at 532 nm. All ELDA profiles were obtained with automated smoothing with maximum allowable relative errors of 20% and 50% below and above 2 km, respectively.

parameter. Thus, this uncertainty does not depend on the errors that are attributed to the signal values. Instead, it reflects the deviation of single data points within the fit window from the fitted line. On the other hand, the uncertainty derived by Monte Carlo method comes directly from the errors of the used signals and is independent on the applied extinction retrieval method.

3.4 Quality control

5   During the automated quality control, each data point of the derived product is inspected. If the absolute value of a negative data point is larger than twice its statistical uncertainty (2σ criterion), this data point is labeled as *invalid*. When writing results to the NetCDF output file, those invalid data points are replaced by the corresponding NetCDF fill value.

Further, all data points below minimum and above maximum altitude are considered as *invalid*. The maximum altitude is the altitude up to which the corresponding product can be derived under optimal atmospheric conditions. It usually depends on

10   hardware parameters like laser power, telescope size, or background suppression. The minimum altitude of the products 'elastic backscatter coefficient' , 'extinction coefficient', and 'lidar ratio' is the altitude of complete overlap if no overlap correction is performed. If this correction is performed, the user can provide a minimum value which corresponds to the altitude down to which the overlap correction profile is trustworthy according to the user's experience. The minimum altitude of the 'Raman backscatter coefficient' product is the altitude down to which the overlap profiles of both signals are equal and cancel out

15   during the retrieval. Both, minimum and maximum altitudes are to be provided by the user for each individual product.

In case of backscatter retrievals with the Klett-Fernald algorithm, all data points above the actual calibration window are considered invalid because the results of the Klett-Fernald method in forward integration mode often is not stable Klett (1981).

Forward integration region is starting from the calibration point and propagating away from the lidar. The actual calibration window is the lowest one (closest to the lidar) of all calibration windows that were found during the Monte Carlo process.

4 ELDA specific algorithms

4.1 Implementation of automated vertical smoothing and temporal averaging

5 ELDA allows for the automated vertical smoothing and temporal averaging of the derived products. The user has the option to adjust the degree of smoothing and averaging of each individual product by setting several parameters. In general, those parameters and constraints can be defined for two different altitude regions, below and above 2 km altitude. Two threshold values for the maximum allowable relative statistical error of the product below and above 2 km altitude can be defined. This separation corresponds to typical atmospheric conditions with large particle extinction coefficients and particle backscatter

10 coefficients within the planetary boundary layer and smaller α and β values above. Usually, profiles within the planetary boundary layer (PBL) can be retrieved with smaller uncertainties than profiles in the clean free troposphere. The separation height of 2 km corresponds to typical top heights of PBL. Further, the user can provide detection limits. Those are absolute values and have the same unit as the product they refer to. Values of extinction coefficients and backscatter coefficients in atmospheric layers characterized by a low aerosol load are close to zero and the relative uncertainties easily can have values of

15 several hundreds percent even if the absolute uncertainties of the data are small. In those cases, if an extinction or backscatter value is smaller than the corresponding detection limit, not the relative uncertainty but absolute uncertainties are used to check whether the degree of smoothing or averaging is sufficient.

Beside these user defined constraints, there are fixed limitations concerning the maximum allowable smoothing and averaging. It is not allowed to apply a smoothing that would result in effective vertical resolutions larger than 500 m and 2 km

20 below and above 2 km altitude, respectively. Further, it is not allowed that size of the smooth window (diameter of smoothing cell) changes by more than 3 bins between two neighboring altitude bins of the profile. According to EARLINET rules, the minimum and maximum allowable averaging times in both altitude regions are 30 minutes and 2 hours, respectively.

The degree of smoothing is determined by the number of data points within the fit window and within the sliding average window in case of extinction and Raman backscatter retrievals, respectively. For the calculation of backscatter profiles with the

25 Klett-Fernald method, no smoothing procedure has been implemented yet.

Automated vertical smoothing is implemented as an iterative procedure: in an initial step, the product is calculated with the maximum allowable vertical smoothing. In the following steps, the algorithm checks for each range bin of the profile whether the relative statistical uncertainty is below the user defined maximum allowable uncertainty or if the absolute uncertainty is below the user defined detection limit. If yes, the radius of the corresponding smoothing cell is reduced by one bin. In order to

30 avoid artificial gradients in the smoothed profile, this step is not allowed if the difference between the smoothing cells of two neighboring bins would become larger than 3 bins. Then the profile is recalculated. The reduction of smoothing (if possible within the allowed uncertainty constraints) and the recalculation are repeated until no further improvements of the vertical resolution are possible.
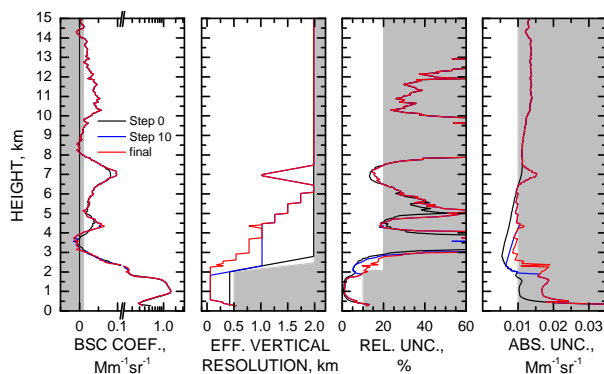
Figure 3. Illustration of the automated smoothing procedure. The example Raman backscatter profile at 532 nm was measured on May 28 between 20:09 and 20:24 UT in Leipzig with the MARTHA lidar. Panels from left to right show the particle backscatter coefficient, the effective vertical resolution, the relative statistical uncertainty, and the absolute statistical uncertainty. Gray areas show constraints of the smoothing procedure and of the uncertrainties, the black, blue, and red curves show the initial maximum smoothing, the status after 8 iteration steps, and the final result (after 16 iteration steps), respectively.

Figure 3 illustrates this algorithm using an example measurement which was obtained during EARLI09 (Wandinger et al., 2015) with the MARTHA instrument (Mattis et al., 2002). The maximum allowable relative uncertainties are 10% and 20% below and above 2 km altitude, respectively, with a detection limit of $1 \times 10^{-8} \mathrm{m}^{-1} \mathrm{sr}^{-1}$. Up to an altitude of about 7.5 km, the vertical resolution of almost all data points are reduced compared to the initial maximum smoothing. The absolute uncertainty

5 is larger than $1 \times 10^{-8} \mathrm{m}^{-1} \mathrm{sr}^{-1}$ below 2.5 km altitude, but smoothing could be reduced because the relative uncertainty is smaller than the allowed 10% or 20%. Between 2.5 and 6 km altitude, smoothing could be reduced because absolute uncertainty stays below the detection limit. Above 7.5 km altitude, both uncertainty thresholds are exceeded, but smoothing could not be increased because it is required to keep the effective vertical resolution smaller than 2 km.

The automated temporal averaging is implemented in a similar way. The intermediate files contain time-series of the pre-

10 processed signal profiles (time slices). In an initial step, the product is derived from the first time slice of the time series. Then it is validated whether the averaging time of the product is larger than the minimum averaging time (30 minutes) and whether the uncertainty constraints are fulfilled for each data point in the altitude range between minimum and maximum altitude of the product (see section3.4). If one of these conditions is not fulfilled, an averaged signal is derived from the first and second time slice profile and the product is recalculated. This procedure is repeated until there are no more time slices in the intermediate

15 file or until the maximum allowable averaging time is exceeded or until either the relative or the absolute uncertainty is below the threshold for all data points of interest (between user defined minimum and maximum altitude). If there are further time slices in the intermediate file, a next, automatically smoothed and averaged product profile is created.

Figure 4 illustrates the averaging algorithm using the same example as before. In this example, the length of the time slices is 15 minutes. The first product profile is the result of the previously described automated smoothing procedure. It cannot be
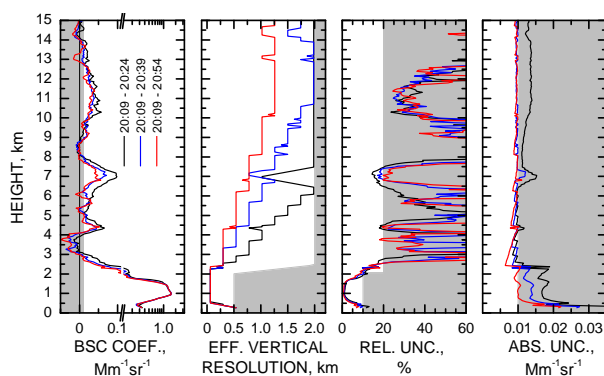
Figure 4. Illustration of the automated averaging procedure. The example Raman backscatter profile at 532 nm was measured at May 28 between 20:09 and 20:54 UT in Leipzig with the MARTHA lidar. Panels from left to right show the particle backscatter coefficient, the effective vertical resolution, the relative statistical uncertainty, and the absolute statistical uncertainty. Gray areas show constraints of the smoothing procedure and of the uncertrainties, the black, blue, and red curves show the averaging periods from 20:09 to 20:24, 20:39, and 20:54 UT, respectively.

used as result because its averaging time is too short and both, relative and absolute uncertainties are above the thresholds below 500 m and above 7.5 km altitude. Next, the 30-minute-profile is almost perfect. There is only one data point around 2 km altitude which does not fulfill the uncertainty criteria. Finally, the 45-minute profile meets all requirements. Further, the increase of averaging time by a factor of three leads to a significant improvement of effective vertical resolution. Whereas

5   uncertainties remain very similar, the length of the smooth windows above 2.5 km altitude is almost half as large as for the 15-min product.

4.2   Handling of effective vertical resolution and lidar ratio calculation

Some data handling procedures like vertical smoothing or the calculation of particle extinction coefficients with Raman method influence the effective range resolution of the retrieved profile. Even if the resulting profiles are reported with the same range

10   resolution as the input data profiles, those procedures cause a loss of information and the resulting range resolution is lower than the original one. The relation between the original and the resulting (effective) range resolution depends on the kind of the applied data handling procedures and on the number of data points which are included in the analysis. These relations were determined by a step function method using the Rayleigh criterion for ELDA's smoothing and extinction procedures as explained in Pappalardo et al. (2004). The tested procedures have been applied to synthetic data with two narrow and well-

15   separated peak structures. By changing the distance between the input peak structures, it is possible to find the minimum distance for which the resulting peaks can be resolved according to the Rayleigh criterion. This minimum distance corresponds to the effective range resolution of the retrieved profile.

In case of extinction retrievals, the effective range resolution depends on the number of data points that are used for the calculation of the linear fit (number of used bins n_α) and on the applied fit algorithm. Here, n_α corresponds to the diameter of the smoothing cell. The relation between n_α and the corresponding effective range resolution $\mathrm{d}r_\alpha$ was determined for values of n_α between 3 and 29 for the linear fit method that is used in ELDA. This relation can be approximated by a linear fit

$$\mathrm{d}r_\alpha = (0.775 n_\alpha + 0.83)\,\mathrm{d}r \tag{3}$$

with $\mathrm{d}r$ being the range resolution of the pre-processed intermediate SCC files.

Profiles of ELDA products are calculated with a variable range resolution. In order to allow for an appropriate interpretation of these data, the vertical profile of the effective vertical resolution—which is derived from the profile of the effective range resolution and the lidar pointing angle—is reported as a variable in the output NetCDF file. For this purpose, the new variable 'VerticalResolution' was introduced into the EARLINET netCDF format.

The smoothing of Raman backscatter profiles is based on sliding averages of the ratio between the elastically backscattered signal and the Raman signal (see section 4.1). According to Iarlori et al. (2015), the effective range resolution in this case is

$$\mathrm{d}r_\beta = (2 n_\beta + 1)\,\mathrm{d}r \tag{4}$$

with n_β being the radius of the smoothing window.

The particle lidar ratio S is the ratio between the particle extinction coefficient α and the particle backscatter coefficient β. In order to retrieve a profile of S, one needs to derive the profiles of α and β with the same vertical profile of effective range resolution (Iarlori et al., 2015). Both profiles are first calculated by using ELDA's automated smoothing scheme. In general, the range resolution of backscatter profiles is better than the resolution of the corresponding extinction profiles. Thus, in a second step, backscatter profiles are additionally smoothed with a second order Savitzky-Golay (SG) polynomial filter (Press et al., 1992) in order to achieve the same vertical profile of effective range resolution as the corresponding extinction profile. The relation between the number of altitude bins used for this filter $n_{\beta,SG}$ and the resulting effective range resolution of the backscatter profile $\mathrm{d}r_{\beta,SG}$ was obtained in the same way as for the extinction retrieval

$$\mathrm{d}r_{\beta,SG} = (1.24 n_{\beta,SG} - 0.24)\,\mathrm{d}r. \tag{5}$$

Here, $n_{\beta,SG}$ is the number of Savitzky-Golay coefficients which corresponds to the radius of the smoothing cell, in contrast to n_α which corresponds to the diameter of the smoothing cell. The previous sliding average smoothing of the signal ratio does not significantly effect the resulting effective range resolution of the backscatter profile as long as $\mathrm{d}r_{\beta,SG} \geq \mathrm{d}r_\beta$. The behaviour in the frequency domain of the applied cascading of sliding average smoothing and second order Savitzky-Golay filtering is simply expressed by the product of the corresponding transfer functions. Moreover the side-lobe issue is generally reduced with the cascade operation (Iarlori et al., 2015).

From equations 4 and 5 and the constraint of $\mathrm{d}r_\alpha = \mathrm{d}r_{\beta,SG}$, the number of Savitzky-Golay coefficients needed for the smoothing of the backscatter profile can be derived from the number of used bins for the extinction smoothing as

$$n_{\beta,SG} = 0.625 n_\alpha + 0.86. \tag{6}$$

Other approaches on the effective resolution handling (e.g., from Iarlori et al. (2015)) will be critically considered in future versions of ELDA.

4.3 Merging of products

Some lidar instruments are equipped with two telescopes. One of them is usually optimized for measurements close to the lidar
5 (near range) and the other one is optimized for measurements at larger altitudes (far range). The SCC is able to derive single atmospheric profiles of particle extinction coefficients and particle backscatter coefficients from signals measured with both telescopes. The SCC Raman backscatter usecases 2, 4, 6, 12, and 13 or extinction usecases 2, 4, and 5 describe the handling of data from those lidar instruments (D'Amico et al., 2015a). First, the signals of each telescope are pre-processed separately by ELPP. Next, those intermediate signals are individually processed and combined at product level by ELDA.
10   The merging of product profiles is done within the 'merge interval'. Its lower boundary is the height of complete overlap of the far-range telescope. The upper boundary of the merge interval is an user-defined parameter.

Merged extinction profiles with automated vertical smoothing are determined with the following steps:

1. Separate calculation of extinction profiles from the pre-processed signals from both telescopes. Both profiles are vertically smoothed with the automated procedure described in section 4.1. The two input signals may have different signal-
15   to-noise ratios at certain altitude ranges. At those altitudes, the resulting extinction profiles will have different effective range resolutions.

2. Thus, a common profile of effective range resolution is generated by using the maximum values of n_α for each range bin. Both profiles are re-calculated with the common, maximum vertical smoothing.

3. The search for the height where both profiles match best is the next step. A window of used-defined width, the 'merge
20   window' is shifted through the merge interval. The window which has the smallest relative mean difference between both profiles is called 'merge region'. The merge point is defined as the center of the final merge region. Additionally, the merge region needs to fulfill all of the following quality criteria:

    (a) Both profiles overlap within the range of their uncertainties.

    (b) Relative statistical uncertainties of both profiles are below the user defined threshold. If the signal-to-noise ratio
25   of a signal is very small, it is possible that the uncertainties are above the threshold even if maximum allowable smoothing was applied. In this case, the tested window would not be appropriate as merge region.

    (c) Both profiles should be parallel. This criterion is tested by comparing the vertical gradients ('slopes') of both profiles. The relative difference between these slopes must be below a user defined threshold. The two slopes are calculated by linear fit of extinction versus altitude.

30 4. Usually, one or both of the profiles obtained from step 2 are over-smoothed in large parts of the merge interval which typically extends over an altitude range of several kilometers. Now, the effective range resolution of both profiles is

reduced to optimum values without causing artifacts due to steplike changes of the range resolution. The resolution within the merge region remains the the effective resolution corresponding to maximum smoothing. There is a steady downward and upward transition from the resolution at the edges of the merge region towards the original resolutions of the near-range and far-range profiles, respectively (see section 4.1). Both profiles are re-calculated with the final vertical resolution.

5. Finally, the data values and uncertainties of the near-range and far-range profiles $x_n(i)$ and $x_f(i)$ are merged into a combined profile $x(i)$ using a sigmoidal weighting function $x(i) = x_n(i)\,[1 - \sigma(i)] + x_f(i)\sigma(i)$. The sigmoidal weighting function $\sigma(i)$ of the range bin i is defined as

$$\sigma(i) = \frac{1}{1 + \exp\left(\frac{i_g - i}{\Delta_g}\right)} \qquad (7)$$

with i_g being the merge point and Δ_g being the vertical scaling of the sigmoidal function. Within ELDA, Δ_g is defined as the number of range bins within the merge region divided by five. Thus, the weight of the near-range profile decreases from 92.4% at the bottom to 7.6% at the top of the merge window. At the merge point, the weighting of both profiles is equal. At half distance between merge point and the edge of the merge region, $\sigma(i)$ has a value of 75% (see figure 6d).

Figures 5 and 6 explain details of this merging procedure with an example measurement which was performed with the PollyXT instrument OCEANET (Engelmann et al., 2015) at Leipzig, Germany, on September 1, 2015 between 0:00 and 1:30 UT. A merge window of 500 m width shall be found within the merge interval which extends from the altitude of full overlap of the far-range telescope at 1 km altitude up to 5 km altitude where the signal-to-noise ratio of the near-range signal of the PollyXT instrument typically becomes too small for data analysis. Even if both extinction profiles were smoothed with the same resolution (see step 2), the statistical uncertainty of the near-range extinction profile is larger than the uncertainty of the far-range profile within the whole merge interval. Conditions 3a and 3b are fulfilled in large parts of the merge interval. Where these conditions are not fulfilled, profiles in panels b) and c) of figure 5 do overlap with gray areas. There are several altitude regions where the slope difference between both profiles is smaller than 50% (condition 3c). The merging algorithm finds the merge window with the smallest distance between both profiles (merge region) at (1.94 ± 0.25) km height. There, near-range and far-range profiles match. Extinction values are almost identical, the profiles are parallel and the uncertainties are below the threshold values.

Figure 6 illustrates the merging procedure itself. The effective vertical resolution of the original far-range profile (step 1) is better than the resolution of the original near-range profile. Both original profiles were automatically smoothed in order to keep relative statistical uncertainties below the threshold value of 30% and 50% below and above 2 km height, respectively. When profiles are obtained with the final vertical smoothing (step 4), the degree of smoothing of the far-range within the merge window is increased until it fits to the stronger smoothing of the original near-range profile. Below and above the merge window, both profiles are smoothed with the original resolution of the near-range and far-range profile, respectively. Where the smoothing of the far-range profile is increased (below 2 km altitude), its uncertainty is decreased. Where the smoothing of the near-range profile is decreased (above 2.3 km altitude), its uncertainty is increased. Between 1.69 and 2.19 km height, the
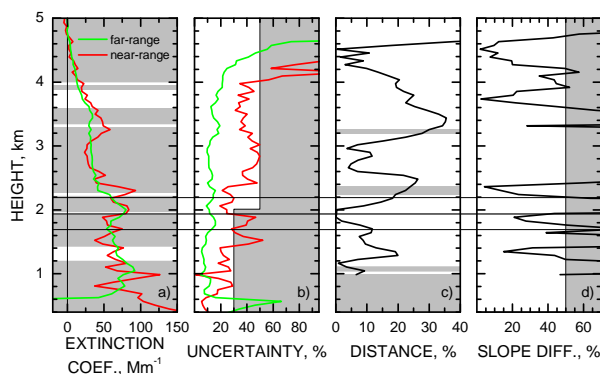
Figure 5. Illustration of the search for the merge region. Red and green curves in a) and b) are the extinction profiles and its relative statistical uncertainties with maximum vertical smoothing. c) and d) show the mean relative distances and slope differences of the moving merge windows. Gray area in b) illustrates the error threshold. Gray areas in c) mark height ranges where the profiles do not overlap within their uncertainties. Gray areas in d) indicate height regions where the slope difference is larger than the threshold of 50%. Gray areas in a) show all height ranges where one or more of the quality criteria of the search for the merge window are not fulfilled. Horizontal thin black lines indicate the position of bottom, center (merge point), and top of the merge window.
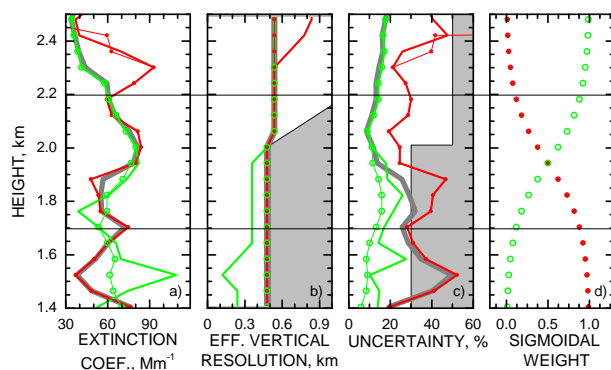
Figure 6. Illustration of the merging procedure. Presented are profiles of particle extinction coefficients (a) with the corresponding effective vertical resolutions (b) and statistical uncertainties (c) as well as the profiles of the sigmoidal weighting factors (d). Red and green curves are the original near-range and far-range profiles, respectively (step 1). Thin red and green curves with symbols correspond to profiles which were calculated with final vertical resolution (step 4). Red dots and green circles in panel (d) show the sigmoidal weighting factors of the near-range and far-range profiles, respectively. Bold gray profiles below the colored lines indicate the final results (step 5). Light gray areas illustrate the constraints of uncertainty and vertical resolution. Horizontal thin black lines indicate bottom and top of the merge window.

extinction profiles and their uncertainty profiles are combined with a sigmoidal weighting function. When averaging both (dotted) profiles, the weight of the near-range profile is decreased and the weight of the far-range profile is increased exponentially. Thus, artificial vertical gradients in the final product profiles can be avoided.

In case of backscatter retrievals, the general procedure is the same. The only difference is that initial near-range and far-range profiles (step 1) are not calculated in parallel. Usually, the signal-to-noise ratio of the near-range profile would be very small at altitude regions where particle free conditions can be assumed. Thus, the far-range profile is calculated first and then it is used for the calibration of the near-range profile. A height window with the same width as the merge window is shifted upward

5   through the merge interval of the far-range profile until the mean backscatter value within this window and its uncertainties fulfill the requirements of a suitable calibration window (see section 3.1.3). This altitude window is then used as calibration window for the retrieval of the corresponding near-range profile. It cannot be assumed that there are aerosol free conditions in this region. Therefore, the actual mean value of the far-range backscatter ratio within this window is used as calibration value instead of the ideal value of backscatter ratio = 1. The following steps 2 to 5 are exactly the same as in the case of retrieval of

10   merged extinction profiles.

4.4   Handling of cloud flags

Cloud-flag data are provided to ELDA within the intermediate files prepared by ELPP. They have the same sampling interval and time resolution as the pre-processed signals. ELDA handles cloud-flag values as byte variables which can have one of the values: 'no cloud'$= 2^0 = 1$ (first bit set), 'cirrus'$= 2^1 = 2$ (second bit set), or 'low cloud'$= 2^2 = 4$ (third bit set). If a data

15   point is attributed to more than one of these categories, all corresponding bits are set in the cloud-flag byte variable. The coarse separation between 'cirrus' and 'low cloud' is made from aerosol-lidar data-analysis point of view. Cirrus clouds are usually characterized by low particle optical depth. Thus, the laser beam is not fully attenuated in the cloud and the signal-to-noise ratio above the cloud is sufficiently large to allow for an analysis of the signals with the usual algorithms and methods. From data-analysis point of view, cirrus clouds behave like aerosol layers in larger altitudes. In contrast, the term 'low clouds'

20   summarizes all clouds which have a large optical depth and completely attenuate the laser beam. At low altitude levels, those are fog, cumulus or stratus clouds. Further, midlevel clouds which contain water droplets belong to this category. If those 'low clouds' occur in a lidar signal profile, usual data analysis algorithms and methods often cannot be applied because the signals may suffer from saturation effects, might be influenced by signal-induced noise, and the signal-to-noise ratio above the cloud is typically too small for backscatter calibration or Raman extinction retrievals.

25   In simple operations, ELDA just copies the cloud-flag values from one data-analysis step to the next one. In case of operations which handle more than one data point (e.g., vertical smoothing, temporal averaging, calculation of mean values, or merging) the cloud-flag data of all involved data points are combined by bitwise logical OR operation. For example, if some data points which are labeled as 'no cloud' and some other data points which are labeled as 'cirrus' are averaged, the resulting cloud-flag value is $3 = 1 + 2$.

30   ELDA does not apply any specific analysis of the cloud-flag data. The corresponding information is just transferred through all analysis steps and is finally reported in the EARLINET *b files* and *e files* as a profile variable __*CloudFlag*. Thus, the user can take the cloud information into account when interpreting the aerosol profiles.

5   Validation

The validity and applicability of SCC has been tested with different approaches. First, D'Amico et al. (2015a) have shown that direct comparisons of single backscatter and extinction profiles retrieved by SCC to profiles which were manually obtained with the individual software of five EARLINET groups are in good agreement with profile mean differences of backscatter and

5   extinction profiles below $1.5 \times 10^{-7} \mathrm{m}^{-1}\mathrm{sr}^{-1}$ and $7 \times 10^{-6} \mathrm{m}^{-1}$, respectively. All of those profiles have been measured at the same time and place with different EARLINET lidar instruments during the EARLI09 campaign in Leipzig (Wandinger et al., 2015).

Further, statistical comparisons of backscatter and extinction profiles based on lidar measurements which were performed at Leipzig and Potenza during several months under different atmospheric conditions showed that there is no systematical bias

10   between manually and SCC retrieved profiles (D'Amico et al., 2015a). Also the comparison of climatological mean lidar ratio profiles and profiles of Ångström exponents show a very good agreement between the manually and SCC retrieved data sets within their uncertainties.

Next, Sicard et al. (2015) report about an experiment around the Mediterranean basin in July 2012. Eleven EARLINET stations performed continuous measurements over a period of 72 hours. This experiment is used as a demonstration for the

15   capability of EARLINET to monitor special events and to deliver SCC products in real time or near real-time. During this period, measured raw data have been uploaded to the SCC automatically and pre-processed signal files in terms of homogenized, range-corrected signals have been delivered by the SCC pre-processing module ELPP in near real-time. From about 75% of these pre-processed data, profiles of backscatter and extinction coefficients could be obtained with the SCC optical module ELDA in near real-time. The remaining measurements are mostly contaminated by clouds.

20   Here, the accuracy of SCC retrieved optical profiles will be tested following the procedure of the EARLINET-ASOS algorithm inter-comparison exercises for elastic backscatter and Raman method (Böckmann et al., 2004; Pappalardo et al., 2004). For this exercise, synthetic elastic and Raman lidar signals were generated with a lidar simulation model. Vertical profiles of particle extinction and backscatter coefficients, particle lidar ratio, pressure and temperature were used as input data for this model. Participating EARLINET groups analyzed the synthetic signals with their own algorithms in several stages. First, the

25   ability of participating algorithms to handle typical atmospheric situation was tested. In this case, usually only measured signals and ground values of temperature and pressure were known. In a last stage, all necessary input parameters like profiles of pressure, temperature and lidar ratio together with calibration information for the backscatter retrievals were revealed. In this stage, the accuracy of the tested algorithms in terms of numerical correctness and stability was validated. Those studies have been performed within EARLINET several times. Here, we use the signals which were simulated for the inter-comparison

30   exercise for new groups in the framework of EARLINETASOS (Böckmann and Pappalardo, 2007).

Table 1 provides an overview on all possible combinations of retrieval methods and the both methods of uncertainty retrieval implemented in the SCC. All of these algorithms and methods were tested in this validation exercise. All input parameters were known as in the last stage of the algorithm inter-comparison exercise. The only exception is the overlap-correction function which was not provided. The pre-processing module ELPP generated range-corrected, pre-processed signals from the synthetic

elastic signals at 355, 532, and 1064 nm as well as from the corresponding synthetic Raman signals at 387 and 607 nm. These intermediate SCC files contain also profiles of the atmospheric transmission and of the molecular scattering coefficient at all corresponding wavelengths which were calculated from the known input profiles of temperature and pressure.

Figure 7 illustrates the simulated atmospheric conditions. Input data of the simulation are plotted with bold lines. The planetary boundary layer (PBL) with large values of particle backscatter and extinction coefficients extends up to 1.5 km. The layer between 1.5 and 3 km altitude is a clean area in the free troposphere (FT) which is characterized by very small backscatter and extinction values. On top of this clean layer—between 3 and 7 km altitude—is a lofted layer (LL) as it typically can be observed during events of long-range transport of aerosol particles.

Figures 8 to 12 provide an overview on relative and absolute deviations between all SCC products and the corresponding simulation input profiles. Simulation input profiles are treated as the truth. The deviations has been calculated as mean values in the altitude regions PBL, FT, and LL. The deviations in the PBL layer does not include data below 0.5 km altitude because the simulated signals are affected there by an incomplete overlap between laser beam and telescope field-of-view. In general, the SCC modules are able to apply an overlap correction to the submitted raw signals if the user provides corresponding overlap-correction function together with the raw data. Unfortunately, this feature could not be tested in this validation exercise because the overlap-correction function was not known.

For a quantitative evaluation of the quality of the products, the three parameters mean deviation $\overline{d}$, mean relative deviation $\overline{d_r}$, and normalized root-mean-square deviation $nRMSD$ were calculated for each product and layer. They are defined as

$$\overline{d} = \langle x_i - s_i \rangle, \tag{8}$$

$$\overline{d_r} = \left\langle \frac{x_i - s_i}{s_i} \right\rangle \times 100, \text{ and} \tag{9}$$

$$nRMSD = \sqrt{\left\langle (x_i - s_i)^2 \right\rangle} \, \langle s_i \rangle^{-1} \times 100 \tag{10}$$

where x_i and s_i are the values of the SCC retrieved and simulation input profiles at range bin i, respectively. $nRMSD$ is a measure for the amplitude of the random fluctuation of the SCC retrieved profile around the true profile. In contrast, $\overline{d}$ and $\overline{d_r}$ describe the systematic deviation between both profiles. In layers with low backscatter and extinction values, relative deviation can easily reach a few hundred percent even if the absolute deviation is really small. Therefore, we discuss the accuracy achieved with SCC products not only in terms of percentage deviations but also in terms of absolute deviations.

Figure 8 gives a summary of the quality of the SCC extinction methods. In case of particle extinction coefficients which are retrieved with the same extinction method but with different methods for the uncertainty retrieval, the extinction profiles and thus the deviations are identical. The resulting products differ only slightly in terms of the estimated uncertainties.

All absolute deviations are smaller than $20 \times 10^{-6} \text{m}^{-1}$ within the PBL and smaller than $7 \times 10^{-6} \text{m}^{-1}$ in the FT and LL altitude regions. Both values are clearly below the maximum allowed deviation of extinction coefficients $(5 \times 10^{-5} \text{m}^{-1})$

according to the EARLINET quality requirements (Matthias et al., 2004). This result is also comparable to the deviations of 11 individual algorithms of different EARLINET groups that have been found in the first algorithm inter-comparison exercise carried out in 2003 (Pappalardo et al., 2004). The atmospheric condition simulated for the previous exercise was different but similar to the situation in this study. It also consisted of a PBL with a clear layer and a lofted layer above.

5 There is a systematic underestimation of particle extinction coefficients in the lowest layer. The reason for this behavior could be a contamination with lower values in the region of incomplete overlap and / or with lower values in the clean free troposphere above 1.5 km due to smoothing. Relative deviations are on average 8%, but always smaller than 12% and thus, they are again smaller than the maximum allowed value of 20%. Relative deviations in the previous exercise were within 10% in the PBL and within 20% in a lofted layer for most of the inter-compared algorithms (Pappalardo et al., 2004).

10 The $nRMSD$ as measure for the fluctuations is about 20% for PBL values at 355 nm but up to 55% elsewhere. Here, the SCC retrievals do not meet the EARLINET requirement of 25% (Matthias et al., 2004). But, the maximum allowed absolute value of $1 \times 10^{-4} \mathrm{m}^{-1}$ is larger than the fluctuation of the SCC results of 3×10^{-5}, 1×10^{-5}, and $3 \times 10^{-5} \mathrm{m}^{-1}$ (2×10^{-5}, 1×10^{-5}, and $2 \times 10^{-5} \mathrm{m}^{-1}$) at 355 nm (532 nm) in the PBL, FT, and LL, respectively. Similar results with fluctuations of 25% in the PBL and of up to 50% in the LL have been found in the previous exercise (Pappalardo et al., 2004).

15 Figures 9, 10, and 11 illustrate the quality of the SCC methods for the retrieval of particle backscatter profiles from elastic signals only (elastic backscatter) and from a combination of elastic signal and Raman signal (Raman backscatter). All profiles have been calculated with the automated calibration procedure as it is described in section 3.1.3 with the following parameters: width of the calibration window is 1 km, the search range for calibration is between 5 and 10 km and it is assumed that the mean backscatter ratio in the calibration window is 1. The automated smoothing procedure shall retrieve profiles with relative uncertainties below 10% or 20% below or above 2 km altitude with a detection limit of $1 \times 10^{-7} \mathrm{m}^{-1} \mathrm{sr}^{-1}$.

20 According to the EARLINET requirements, errors of backscatter coefficients at 355 and 532 nm (1064 nm) have to be below 20% (30%) or smaller than $5 \times 10^{-7} \mathrm{m}^{-1} \mathrm{sr}^{-1}$ (Matthias et al., 2004). Relative deviations of the SCC backscatter products are on average 10%, but show a large variability between wavelengths and methods. The Raman backscatter coefficients at 355 nm have deviations of 30% in the FT, but absolute deviations of about $1.5 \times 10^{-7} \mathrm{m}^{-1} \mathrm{sr}^{-1}$ meet the requirements. Largest deviations at 355 nm occur in case of the Klett-Fernald method with input of the correct lidar-ratio profile *KF LRp MC*. $\overline{d_r}$ of $\pm 50\%$ in the FT and LL are very large. But also in this case, absolute deviations meet the requirements. At 532 nm, largest relative deviations of 30% occur in the FT for iterative methods with an input of a fixed lidar-ratio value. At 1064 nm, all $\overline{d_r}$ and $\overline{d}$ meet the requirements. Maximum allowed variations are 25% at 355 and 532 nm, 30% at 1064 nm or $5 \times 10^{-7} \mathrm{m}^{-1} \mathrm{sr}^{-1}$ at all wavelengths. This requirement is fulfilled by all algorithms, at all wavelengths, and in all altitude layers.

30 As already explained in section 3.3, the estimated uncertainty in the PBL is increased if the uncertainty of the lidar-ratio estimation is included in the MC error simulation (methods *it fLR MC2* and *KF fLR MC2*) compared to the methods *it fLR MC* and *KF fLR MC* which ignore this source of uncertainty. This effect is largest at 355 nm and smallest at 1064 nm. Further, the effect of uncertainty amplification in the error propagation of the iterative method is visible by comparing the *it fLR* and *it LRp* with the corresponding *it fLR MC* and *it LRp MC* methods which do not suffer from this error amplification. This effect

35 is larger in PBL and is strongest at 532 nm.
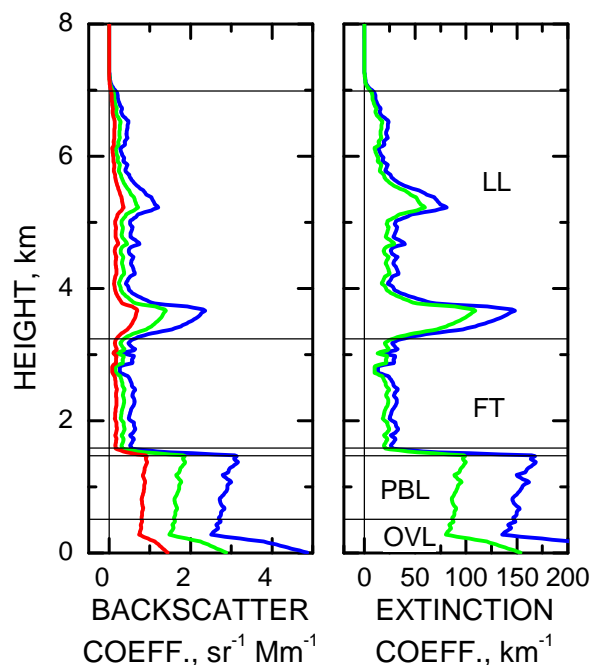
Figure 7. Input data of the algorithm inter-comparison exercise. Profiles of particle backscatter (left) and extinction coefficients (right).The colors indicate the wavelengths: Blue corresponds to 355 nm, green to 532 nm, and red to 1064 nm. Horizontal black lines indicate the layers PBL, FT, and LL where the layer mean deviations of figures 8 to 12 have been derived.

Finally, figure 12 illustrates the performance of the SCC lidar ratio retrievals. There are no EARLINET quality requirements concerning maximum allowed LR uncertainties yet. All deviations are below 15% and 10 sr (5 sr) at 355 nm (532 nm).

6   Conclusions

ELDA is the optical processor module of the SCC. It is a software package that retrieves profiles of particle backscatter
5   coefficients that are derived from an elastic signal only or from a combination of an elastic signal and a Raman signal as well
as profiles of particle extinction coefficients with the Raman method in an automatic way and without the need for operator
interaction.

An expert group performed a survey among the EARLINET groups in order to compile a list of all algorithms used in the
community and to collect individual solutions for critical calculus subsystems. All reported algorithms and methods have been
10   reviewed with respect to their general applicability for the automated algorithms of the SCC software. The expert group decided
which algorithms should be implemented in ELDA. In some cases, if several suitable solutions for one specific problem are
widely used in the community, they were implemented in the software code as parallel options allowing the user to choose

Table 1. List of product types, methods and options for uncertainty retrievals implemented in ELDA. In the validation exercise, all of those products have been tested for 355 and 532 nm (see figures 8-10, and 12). For 1064 nm, only the products listed under 'elastic backscatter coefficient' have been tested (see figure 11).

elastic backscatter coefficient			
id	method	lidar ratio input option	uncertainty retrieval
it fLR	iterative method	fixed value	error propagation
it fLR MC	iterative method	fixed value	MC variation of signal
it fLR MC2	iterative method	fixed value	MC variation of signal and lidar ratio value
it LRp	iterative method	input profile of simulation	error propagation
it LRp MC	iterative method	input profile of simulation	MC variation of signal
KF fLR MC	Klett Fernald	fixed value	MC variation of signal
KF fLR MC2	Klett Fernald	fixed value	MC variation of signal and lidar ratio value
KF LRp MC	Klett Fernald	input profile of simulation	MC variation of signal

Raman backscatter coefficient		
id	method	uncertainty retrieval
R	Raman, via backscatter ratio	error propagation
R MC	Raman, via backscatter ratio	MC variation of signal

extinction coefficient		
id	method	uncertainty retrieval
nwf	non-weighted linear fit	uncertainty of the fit result
nwf MC	non-weighted linear fit	MC variation of signal
wf	weighted linear fit	uncertainty of the fit result
wf MC	weighted linear fit	MC variation of signal

lidar ratio			
id	extinction method	backscatter method	uncertainty retrieval
nwf	nwf	R	uncertainty of the fit result and error propagation
wf	wf	R	uncertainty of the fit result and error propagation
nwf MC	nwf MC	R MC	MC variation of signal
wf MC	wf MC	R MC	MC variation of signal
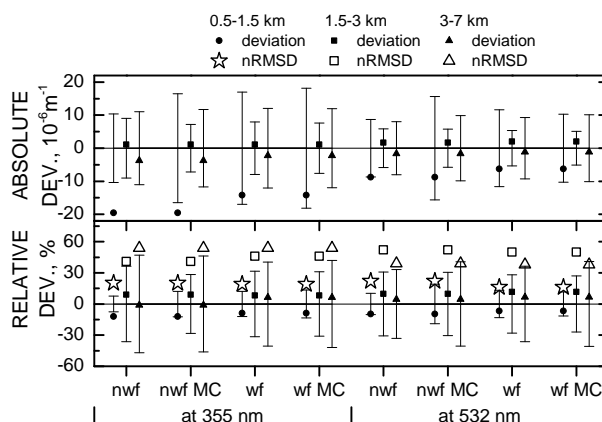
Figure 8. Layer mean absolute (top) and relative (bottom) deviations between particle extinction coefficient profiles at 355 and 532 nm calculated with ELDA and the simulation input profile for three different altitude regions (filled symbols). Open symbols show the root-mean-square deviation which was normalized with the mean value of the input profile (nRMSD). Error bars show the layer mean values of the ELDA derived profiles of absolute and relative statistical uncertainties. The tested methods are identified by short id's corresponding to table 1.
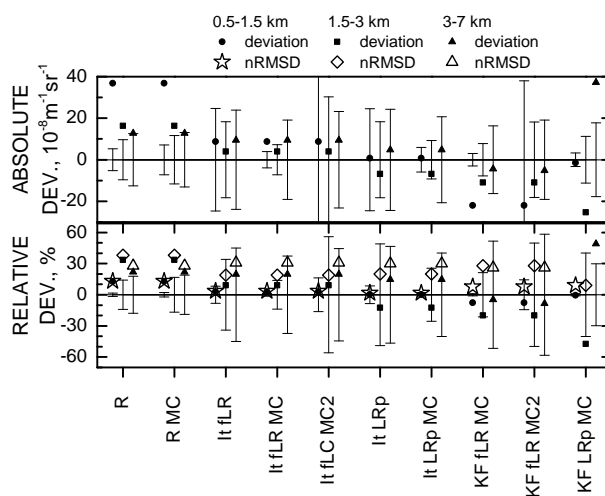
Figure 9. Same as figure 8 but for particle backscatter coefficient profiles at 355 nm. The fixed lidar ratio value was set to 51 sr with an uncertainty of ±10 sr.
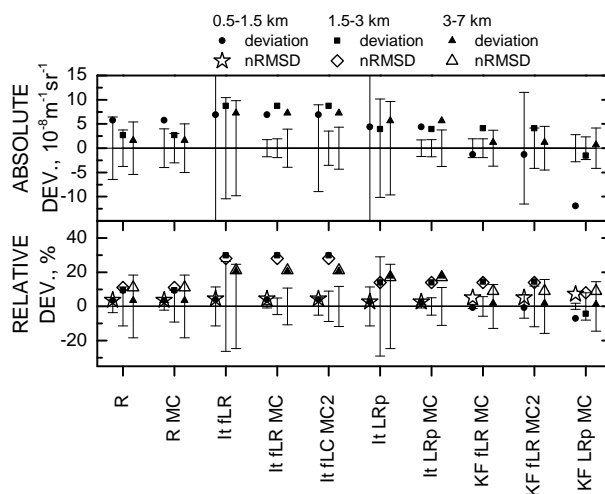
Figure 10. Same as figure 9, but for particle backscatter coefficient profiles at 532 nm and with fixed lidar ratio values of 62 ± 10 sr.
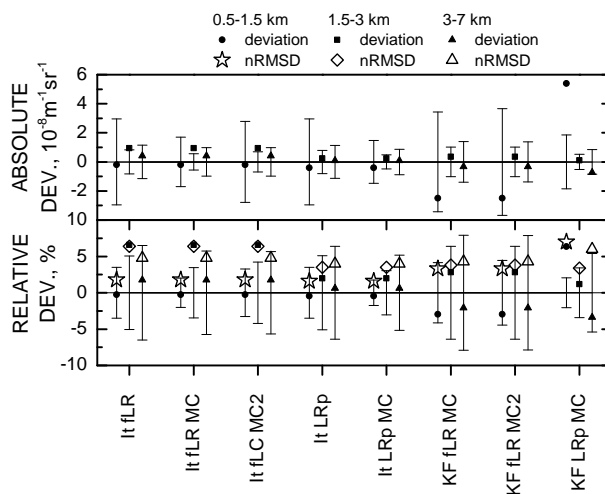
Figure 11. Same as figure 9, but for particle backscatter coefficient profiles at 1064 nm and with fixed lidar ratio values of 85 ± 10 sr. Raman profiles are not available for this wavelength.
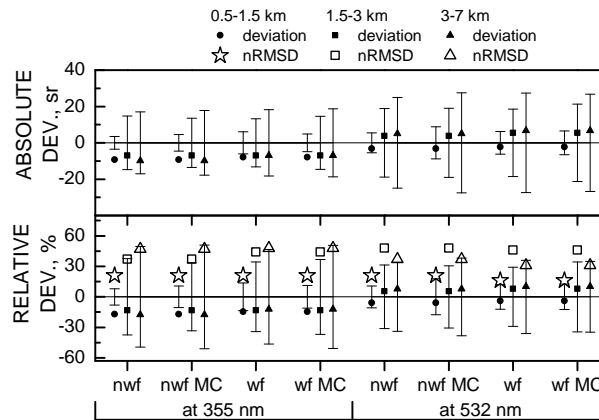
Figure 12. Same as figure 8, but for particle lidar ratio profiles.

among them. Further, it was decided to design the SCC software in a modular way that is easily possible to implement additional algorithms or new optional methods in future.

Main source of input to ELDA are intermediate SCC NetCDF files. They contain lidar signal data which were pre-processed by the SCC module ELPP, profiles of the molecular scattering coefficients, and frequently changing input parameters for the

5   data analysis. Permanent product calculation options are extracted from the SCC relational database. ELDA results are written into NetCDF files strictly following the EARLINET rules. ELDA can automatically be started by the SCC daemon module or manually using the command line interface.

All retrieval algorithms implemented in ELDA are well known in the lidar community, well documented in various publications and well tested in many applications. Some methods and algorithms have been especially developed or adopted for

10   ELDA. Those are the automated vertical smoothing and temporal averaging, the handling of effective vertical resolution in case of lidar ratio calculation, and the merging of product profiles in case of measurements with near-range and far-range telescopes.

ELDA allows for the automated vertical smoothing and temporal averaging of the derived products. The user has the option to adjust the degree of smoothing and averaging of each individual product by setting a detection limit and threshold values for the maximum allowable relative statistical error. The relation between the degree of smoothing in terms of number of height

15   bins and the corresponding effective range resolution was determined by a step function method using the Rayleigh criterion. In order to retrieve a profile of particle lidar ratio , one needs to derive a Raman backscatter profile which has the same vertical profile of effective range resolution as the corresponding extinction profile. In general, the range resolution of backscatter profiles is better than the resolution of the corresponding extinction profiles. Therefore, automatically smoothed backscatter profiles are additionally smoothed with a second order Savitzky-Golay filter in order to derive backscatter profiles which has

20   the same effective range resolution as the corresponding extinction profiles.

In case of lidar systems with two different telescopes for near range and far range, ELDA calculates extinction and backscatter profiles from the signals of both telescopes separately. The final product profile is composed of near-range data and the

far-range data below and above the point of closest match between these profiles, respectively. In case of backscatter retrievals, only far-range signals are used for the calibration.

The accuracy of retrieved optical profiles was tested following the procedure of the EARLINET-ASOS algorithm inter-comparison exercises for elastic backscatter and Raman method. All algorithms and methods which are implemented in the

5 SCC were tested with all input parameters known as in the last stage of the algorithm inter-comparison exercise. For a quantitative evaluation of the quality of the products, mean deviations, mean relative deviations, and normalized root-mean-square deviations were calculated for each product and three altitude layers. No deviations have been calculated below 0.5 km altitude because in this range the simulated signals are affected by an incomplete overlap between laser beam and telescope field-of-view. In the simulated situation, the layer between 0.5 and 1.5 km is representative for the planetary boundary layer, the layer

10 between 1.5 and 3 km altitude is a clean area in the free troposphere, and between 3 and 7 km altitude there is a lofted layer as it typically can be observed during events of long-range transport of aerosol particles.

Mean deviations and mean relative deviations of all extinction products in all layers are clearly below the maximum allowed deviations of extinction coefficients ($5 \times 10^{-5}\,\mathrm{m}^{-1}$ or 20%) according to the EARLINET quality requirements. Moreover, errors of backscatter coefficients at 355 and 532 nm (1064 nm) have to be below 20% (30%) or smaller than $5 \times 10^{-7}\,\mathrm{m}^{-1}\mathrm{sr}^{-1}$.

15 Relative deviations of the SCC backscatter products are on average 10%, but show a large variability among wavelengths and analysis methods. In some cases, the relative deviations are larger than requested, but absolute deviations always meet the requirements. Maximum allowed variations are 25% at 355 and 532 nm, 30% at 1064 nm or $5 \times 10^{-7}\,\mathrm{m}^{-1}\mathrm{sr}^{-1}$ at all wavelengths. This requirement is fulfilled by all algorithms at all wavelengths in all altitude layers. There are not yet EARLINET quality requirements concerning maximum allowed uncertainties of lidar ratio profiles. In case of ELDA retrievals, all deviations are

20 below 15% and 10 sr (5 sr) at 355 nm (532 nm).

The development of ELDA is continuing. Due to its modular structure, new products, usecases, and methods can easily be implemented, e.g. if new, more complex lidar systems are developed or if new products are required from the user community.

Acknowledgements. The financial support for EARLINET in the ACTRIS Research Infrastructure Project by the European Union's Horizon 2020 research and innovation program under grant agreement no 654169 and previously under the grants no 262254 in the 7th Framework

25 Program (FP7/2007-2013) and no 025991 in the 6th Framework Program (FP6/2002-2006) is gratefully acknowledged.

References

Ansmann, A., Riebesell, M., and Weitkamp, C.: Measurement of atmospheric aerosol extinction profiles with a Raman lidar, Opt. Lett., 15, 746–748, 1990.

Ansmann, A., Riebesell, M., Wandinger, U., Weitkamp, C., Voss, E., Lahmann, W., and Michaelis, W.: Combined Raman elastic–backscatter lidar for vertical profiling of moisture, aerosol extinction, backscatter, and lidar ratio, Appl. Phys. B, 55, 18–28, 1992a.

Ansmann, A., Wandinger, U., Riebesell, M., Weitcamp, C., and Michaelis, W.: Independent measurement of extinction and backscatter profiles in cirrus clouds by using a combined Raman elastic-backscatter lidar, Appl. Opt., 31, 7113–7131, 1992b.

Böckmann, C. and Pappalardo, G.: Report on the inter-comparison of algorithms for new stations, Tech. Rep. (Deliverable D3.2), EAR-LINETASOS European Aerosol Research Lidar Network: Advanced Sustainable Observation System, 2007.

Böckmann, C., Bösenberg, J., Wandinger, U., Ansmann, A., Amiridis, V., Boselli, A., Delaval, A., De Tomasi, F., Frioud, M., Grigorov, I., Hågård, A., Horvat, M., Iarlori, M., Komguem, L., Kreipl, S., Larchevêque, G., Matthias, V., Papayannis, A., Pappalardo, G., Rocaden-bosch, F., Rodrigues, A., Schnaider, J., Shcherbakov, V., and Wiegner, M.: Aerosol lidar intercomparison in the framework of EARLINET: Part II - Aerosol backscatter algorithms, Appl. Opt., 43, 977–989, 2004.

Bösenberg, J., Matthias, V., Linné, H., Böckmann, C., Mironova, I., Schneidenbach, L., Kirsche, A., Mekler, A., Wiegner, M., Freudenthaler, V., Stachlewska, I., Kumpf, W., Pappalardo, G., Amodeo, A., Mona, L., Pandolfi, M., Balis, D., Amoiridis, V., Zerefos, C., Ansmann, A., Mattis, I., Wandinger, U., Müller, D., Spinelli, N., Wang, X., Boselli, A., Chaikovsky, A., Comeron, A., Rocadenbosch, F., Pérez, C., Baldasano, J., Pelon, J., Sauvage, L., Perrone, R. M., de Tomasi, F., Eixmann, R., Mitev, V., Matthey, R., Hagard, A., Persson, R., Carlsson, G., Rizi, V., Iarlori, M., Vaughan, G., Trickl, T., Kreipl, S., Giehl, H., Simeonov, V., Resendes, D. P., Rodrigues, J. A., Sobolewski, P., Nickovic, S., Music, S., Zavrtanik, M., Stoyanov, D., Grigorov, I., Kolarov, G., and Papayannis, A.: EARLINET: A European Aerosol Research Lidar Network to Establish an Aerosol climatology, Tech. Rep. 348, Max-Planck-Institut für Meteorologie, Hamburg, 2003.

D'Amico, G., Amodeo, A., Baars, H., Binietoglou, I., Freudenthaler, V., Mattis, I., Wandinger, U., and Pappalardo, G.: EARLINET Single Calculus Chain – overview on methodology and strategyy, Atmos. Meas. Tech., 8, 4891–4916, doi:10.5194/amt-8-4891-2015, 2015a.

D'Amico, G., Amodeo, A., Mattis, I., Freudenthaler, V., and Pappalardo, G.: EARLINET Single Calculus Chain – technical – Part 1: Pre-processing of raw lidar data, Atmos. Meas. Tech. Discuss., 8, 10 387–10 428, doi:10.5194/amtd-8-10387-2015, 2015b.

Di Girolamo, P., Ambrico, P. F., Amodeo, A., Boselli, A., Pappalardo, G., and Spinelli, N.: Aerosol Observations by Lidar in the Nocturnal Boundary Layer, Appl. Opt., 38, 4585–4595, 1999.

EARLINET-ASOS: Final report, Tech. rep., European Aerosol Research Lidar Network: Advanced Sustainable Observation System, 2011.

Engelmann, R., Kanitz, T., Baars, H., Heese, B., Althausen, D., Skupin, A., Komppula, M., Stachlewska, I., Marinou, E., Mattis, I., Linné, H., and Ansmann, A.: EARLINET Raman Lidar Polly^{XT}: The NeXT Generation, Atmos. Meas. Tech. Discuss., 8, 7737–7780, doi:10.5194/amtd-8-7737-2015, 2015.

Fernald, F. G.: Analysis of atmospheric lidar observations: some comments, Appl. Opt., 23, 652–653, 1984.

Ferrare, R. A., Melfi, S. H., Whiteman, D. N., Evans, K. D., and Leifer, R.: Raman lidar measurements of aerosol extinction and backscat-tering: 1. Methods and comparisons, J. Geophys. Res., 103, 19 663–19 672, 1998.

Freudenthaler, V.: About the effects of polarising optics on lidar signals and the Δ90-calibration, Atmos. Meas. Tech. Discuss., doi:doi:10.5194/amt-2015-338, 2015.

Freudenthaler, V., Linné, H., Chaikovski, A., Rabus, D., and Groß, S.: EARLINET lidar quality assurance tools, Atmos. Meas. Tech. Discuss., p. in preparation, 2016.

Iarlori, M., Madonna, F., Rizi, V., Trickl, T., and Amodeo, A.: Effective resolution concepts for lidar observations, Atmos. Meas. Tech. Discuss., 8, 5157–5176, doi:10.5194/amt-8-5157-2015, 2015.

Klett, J. D.: Stable analytic inversion solution for processing lidar returns, Appl. Opt., 20, 211–220, 1981.

Masci, F.: Algorithms for the inversion of lidar signals: Rayleigh-Mie measurements in the stratosphere, Annali di Geofisica, 42, 71–83, 1999.

Matthias, V., Balis, D., Bösenberg, J., Eixmann, R., Iarlori, M., Komguem, L., Mattis, I., Papayannis, A., Pappalardo, G., Perrone, M. R., and Wang, X.: Vertical aerosol distribution over Europe: Statistical analysis of Raman lidar data from 10 European Aerosol Research Lidar Network (EARLINET) stations, J. Geophys. Res., 109, doi:10.1029/2004JD004 638, 2004.

Mattis, I., Ansmann, A., Althausen, D., Jaenisch, V., Wandinger, U., Müller, D., Arshinov, Y. F., Bobrovnikov, S. M., and Serikov, I. B.: Relative humidity profiling in the troposphere with a Raman lidar, Appl. Opt., 41, 6451–6462, 2002.

Mattis, I., Chaikovsky, A., Amodeo, A., D'Amico, G., and Pappalardo, G.: Assesment report of existing calculus subsystems used within EARLINET-ASOS, Tech. rep., EARLINET-ASOS, 2007.

Pappalardo, G., Amodeo, A., Pandolfi, M., Wandinger, U., Ansmann, A., Bösenberg, J., Matthias, V., Amiridis, V., deTomasi, F., Frioux, M., Iarlori, M., Komguem, L., Papayannis, A., Rocadenbosch, F., and Wang, X.: Aerosol lidar intercomparison in the framework of the EARLINET project. 3. Raman lidar algorithm for aerosol extinction, backscatter, and lidar ratio, Appl. Opt., 43, 5370–5385, 2004.

Pappalardo, G., Mona, L., D'Amico, G., Wandinger, U., Adam, M., Amodeo, A., Ansmann, A., Apituley, A., Alados Arboledas, L., Balis, D., Boselli, A., Bravo-Aranda, J. A., Chaikovsky, A., Comeron, A., Cuesta, J., De Tomasi, F., Freudenthaler, V., Gausa, M., Giannakaki, E., Giehl, H., Giunta, A., Grigorov, I., Groß, S., Haeffelin, M., Hiebsch, A., Iarlori, M., Lange, D., Linné, H., Madonna, F., Mattis, I., Mamouri, R.-E., McAuliffe, M. A. P., Mitev, V., Molero, F., Navas-Guzman, F., Nicolae, D., Papayannis, A., Perrone, M. R., Pietras, C., Pietruczuk, A., Pisani, G., Preißler, J., Pujadas, M., Rizi, V., Ruth, A. A., Schmidt, J., Schnell, F., Seifert, P., Serikov, I., Sicard, M., Simeonov, V., Spinelli, N., Stebel, K., Tesche, M., Trickl, T., Wang, X., Wagner, F., Wiegner, M., and Wilson, K. M.: Four-dimensional distribution of the 2010 Eyjafjallajökull volcanic cloud over Europe observed by EARLINET, Atmos. Chem. Phys., 13, 4429–4450, doi:10.5194/acp-13-4429-2013, 2013.

Pappalardo, G., Amodeo, A., Apituley, A., Comeron, A., Freudenthaler, V., Linné, H., Ansmann, A., Bösenberg, J., D'Amico, G., Mattis, I., Mona, L., Wandinger, U., Amiridis, V., Alados-Arboledas, L., Nicolae, D., and Wiegner, M.: EARLINET: towards an advanced sustainable European aerosol lidar network, Atmos. Meas. Tech., 7, 2389–2409, doi:10.5194/amt-7-2389-2014, 2014.

Press, W. H., Flannery, B. P., Teukolsky, S. A., and Vetterling, W. T.: Numerical Recipes in FORTRAN: The Art of Scientific Computing, Cambridge University Press, 2 edn., 1992.

Sicard, M., D'Amico, G., Comerón, A., Mona, L., Alados-Arboledas, L., Amodeo, A., Baars, H., Baldasano, J. M., Belegante, L., Binietoglou, I., Bravo-Aranda, J. A., Fernández, A. J., Fréville, P., García-Vizcaíno, D., Giunta, A., Granados-Muñoz, M. J., Guerrero-Rascado, J. L., Hadjimitsis, D., Haefele, A., Hervo, M., Iarlori, M., Kokkalis, P., Lange, D., Mamouri, R. E., Mattis, I., Molero, F., Montoux, N., Muñoz, A., Muñoz Porcar, C., Navas-Guzmán, F., Nicolae, D., Nisantzi, A., Papagiannopoulos, N., Papayannis, A., Pereira, S., Preißler, J., Pujadas, M., Rizi, V., Rocadenbosch, F., Sellegri, K., Simeonov, V., Tsaknakis, G., Wagner, F., and Pappalardo, G.: EARLINET: potential operationality of a research network, Atmos. Meas. Tech., 8, 4587–4613, doi:10.5194/amt-8-4587-2015, 2015.

Wandinger, U., Freudenthaler, V., Baars, H., Amodeo, A., Engelmann, R., Mattis, I., Groß, S., Pappalardo, G., Giunta, A., D'Amico, G., Chaikovsky, A., Osipenko, F., Slesar, A., Nicolae, D., Belegante, L., Talianu, C., Serikov, I., Linné, H., Jansen, F., Apituley, A., Wilson, K. M., de Graaf, M., Trickl, T., Giehl, H., Adam, M., Comerón, A., Muñoz, C., Rocadenbosch, F., Sicard, M., Tomás, S., Lange, D., Kumar, D., Pujadas, M., Molero, F., Fernández, A. J., Alados-Arboledas, L., Bravo-Aranda, J. A., Navas-Guzmán, F., Guerrero-Rascado,

J. L., Granados-Muñoz, M. J., Preißler, J., Wagner, F., Gausa, M., Grigorov, I., Stoyanov, D., Iarlori, M., Rizi, V., Spinelli, N., Boselli, A., Wang, X., Lo Feudo, T., Perrone, M. R., De Tomasi, F., and Burlizzi, P.: EARLINET instrument intercomparison campaigns: overview on strategy and results, Atmos. Meas. Tech. Discuss., 8, 10 473–10 522, doi:10.5194/amtd-8-10473-2015, 2015.